

PYRO SHOCK SIMULATION: EXPERIENCE WITH THE MIPS SIMULATOR

Thomas J. Dwyer and David S. Moul
GE Astro Space Division, Valley Forge, PA

ABSTRACT

The MIPS (Mechanical Impulse Pyro Shock) Simulator at GE Astro Space Division is one version of a design which is in limited use throughout the Aerospace industry, and is typically used for component shock testing at levels up to 10,000 response g's. Modifications to the force input, table and component boundary conditions have allowed a range of test conditions to be achieved. Twelve different designs of components with weights up to 23 Kg (50 Lb) are in the process or have completed qualification level shock testing in the Dynamic Simulation Lab at GE Astro in Valley Forge, PA. This paper presents a summary of the experience gained through the use of this simulator, and presents examples of shock environments that can be readily simulated at the GE Astro MIPS facility.

INTRODUCTION

The MIPS has been used successfully on numerous programs in the past three years at GE Astro. In general, all testing done to date has been successfully completed with all pre-test objectives satisfied. Achieving the desired Shock Response Spectrum (SRS) for 12 different component designs requires a dedicated and innovative test staff, as well as a thorough understanding of the MIPS facility.

The GE Astro MIPS test setup is illustrated by Figure 1. Components are mounted to a 122 cm x 183 cm x 1.3 cm (4' x 6' x 1/2") thick 7075-T6 aluminum plate, which rests on a 7.6 cm (3") thick foam pad. The shock is generated via the impact of a pneumatic actuator which is rigidly attached to a moveable bridge. The bridge is secured to the table frame at the desired position, which typically places the impact point within 15 cm (6") of the component. Instrumentation location varies depending on the test objectives, but the usual control point is less than 5.1 cm (2") from the component on a line between the impact point and the test specimen. A typical triaxial accelerometer response for the control point is shown in Figure 2, along with the time history of the shock pulse.

The data to date indicates that the MIPS test environment is relatively consistent from test to test. Because pyrotechnic shock results from an explosion and is a high frequency phenomena, the actual pyrotechnic shock environment tends to vary considerably from firing to firing. However, comparison of the SRS for all axes indicates that the MIPS results are relatively repeatable. Although there are some exceptions, the MIPS shock environment tends to have less than 10 percent variation from test to test, which is a considerable achievement for these types of environments.

The MIPS at GE Astro has been used to perform shock qualification testing on a wide variety of components. The majority have been flange mounted black boxes with weights up to 23 Kg (50 Lb) but the fabrication styles have ranged from laser welded housings to cast aluminum boxes. The housing fabrication method determines

the stiffness of the structure and affects the response of the MIPS table. One design was constructed of several stacked modules and another included a free-standing antenna. Specific devices instrumented and monitored during test have included printed wire boards (PWB's), gyroscopes, relays and passive dampers. Modifying the boundary conditions of the table determines the response of the table to the shock input, thus allowing a wide range of components to be successfully tested. Several environments that have been simulated are illustrated by Figure 3, with Shock Response Spectrum (SRS) levels of over 40,000 response g's obtained for specific setups.

DYNAMIC MODELS

The use of dynamic models is necessary to prevent damage to flight hardware during setup of the MIPS table. Fine tuning the table to achieve the proper shock response spectrum can often require up to 80 shocks. With different shock profiles and various size boxes, each configuration becomes a unique technical challenge. Since the control point is on the table, the dynamic models must be designed to simulate the effect the box has upon the table. Box weight and mounting style are the most important factors affecting the response of the table to the shock input, but the effect of cables must also be evaluated for each case. The response of a good dynamic model can be within 2 dB of the flight unit as shown in Figure 4.

The box weight can be simulated with separate masses distributed in such a manner as to correspond to lumped masses within the component. Such lumped masses include power supplies and circuit boards. Figure 4 shows the generic dynamic model design developed at GE Astro for dual flange mounted components. Aluminum blocks are currently used for these masses, and the design has been standardized to allow these blocks to be used in several different dynamic models.

The mounting style is the most critical factor that must be simulated. For flange mounted components, the effect can be duplicated via use of thin rails. The weights, which are sized to provide the proper mass distribution, are attached to the rails at locations between the bolts holding the rails to the shock table. The rail should be of a similar material and thickness to the flange. The effect of structural gussets on the component flange may be neglected for shock response simulation, since only the immediate flange will effectively respond to the .0005 second shock pulse.

The effect of cables depends on the quantity and type of the cables. Properly suspended, flexible cables need not be simulated. Rigid and semi-rigid coaxial cables have been found to have a low frequency effect and should always be simulated with the dynamic model. The cable attachment to the model should duplicate the stiffness of the prime mounting configuration.

CASE HISTORIES

For the successful use of the MIPS Simulator, the operator needs to develop an understanding of the nature of the shock response, as well as an appreciation of the effect that various boundary conditions have upon the table. In general, these modifications to the boundary conditions affect either the impact area or the table supports. The following guidelines have been developed at GE Astro and each particular setup employs a combination of these variations to achieve the desired SRS:

<u>Variation</u>	<u>Resultant</u>
Paper (cardboard) under striker.....	Damps high frequencies
Steel plate under striker	Increases high frequencies
Clamp table edges to frame	Shifts resonance lower
Support table on wood blocks	Damps high frequencies
Jackstand under impact point	Reduces low frequencies
Component on transition plate	Attenuates all frequencies
Bags of lead shot on table	Damps high frequencies
Lower striker height	Evenly attenuates entire spectrum
Reduce ram pressure	Unevenly attenuates entire spectrum

The striker has a rounded aluminum head, which can be replaced with various profiles to acquire the proper impact. Buffering the impact point with paper or cardboard limits the high frequency 'ringing' of the table, but, as seen in Figure 5, equivalent thicknesses of paper and cardboard affect the low frequency end of the SRS differently. Combinations of paper and cardboard are often used to achieve the desired damping. Steel, on the other hand, will increase the high frequency content of the spectrum.

The use of a jackstand beneath the impact point reduces the deflection of the MIPS plate. This deflection results in an increased low frequency component to the SRS. Varying amounts of back pressure upon the jackstand will preload the table and can be used to eliminate undesirable low frequency responses. The air pressure driving the ram also has an effect upon the low frequency response of the table as shown in Figure 5. Increased ram pressure deflects the table to a further extent, and will add a 'DC' effect. Ram pressure is adjusted in accordance with jackstand preloading to achieve the desired response.

Clamping the plate edges to the table will effectively shorten the table length and will shift the table resonance accordingly. Supporting the plate on wood (aluminum) blocks above the foam changes the boundary condition from free-free to simply supported. Variations to these and other boundary conditions have allowed the operators of the MIPS at GE Astro to meet every program specification.

Specific case studies typify some of the common problems and solutions for the operator of the MIPS table:

Components A & B are typical aerospace black boxes consisting of multiple mechanical and electrical components coupled with numerous printed wire boards (PWB's) supported within the rigid containers. Integration of passive viscoelastic damping treatments into the design of spacecraft component mounting structures (including PWB's) significantly improves spacecraft reliability. An additional benefit is increased damping in orbit which reduces response to onboard disturbances. Constrained Layer Damping Assemblies (CLDA's) are typically applied in strips running lengthwise across the board with a Viscoelastic Material (VEM) sandwiched between a stiff constraining layer and the board surface. The CLDA is placed to maximize the strain energy in the VEM, although this is not always possible due to PWB component mounting. All PWB's within Components A & B have CLDA's, as well as several other critical box surfaces. A typical PWB with CLDA is shown in Figure 6. A unique Component B feature is that boundary conditions were applied

to several of the PWB's by strips of flexible silicon rubber pads forming the interface between the container bottom and PWB surfaces on some boards.

During the vibration and shock testing, the boxes were internally instrumented for the purpose of determining the internal dynamic environment resulting from the shock application and the effectiveness of the passive damping treatment used to reduce the response of PWB's. The input to the components was characterized by triaxial locations less than 7.6 cm (3") from the component mounting flanges, and the internal and external component responses were measured with microminiature accelerometers. The PWB accelerometers were positioned near the center of the PWB's to measure the vibration normal to the board. The remaining accelerometers were located on the covers and structural bulkhead. A triaxial location was included at the upper corner of the component near the application of the shock to evaluate the amplification of the overall box structure. Additional detailed information is listed in Reference [1].

The general test geometry is illustrated in Figure 7. Two shock applications were applied for each condition illustrated in Figure 7, with functional tests both before and after the shock applications, and no anomalies were detected in any test.

The data summarized in Table 1 and Table 2 provides a definition of the environment within the components resulting from the MIPS simulation of the pyrotechnic environment. They indicate relatively high SRS levels for electronic parts mounted on the PWB's on the order of 1-2000 g's. The PWB's do provide a significant attenuation of the MIPS plate environment which ranged from 6000-13,000 g's, and the component structural environment (3000-7000 g's). This attenuation is expected in view of the relatively low resonant frequency of the PWB's. The PWB's having the lowest resonant frequency typically have the lowest SRS, while PWB's with the higher resonant frequencies had the higher SRS. Responses in these boxes are thought to be typical for similar application throughout the industry and can be scaled for other shock environments by analysts wanting to determine PWB response characteristics for their application.

Component C utilized a box design which consisted of a heavy, cast aluminum container. This design required the mounting bolts to have an excessive grip to pass through the thick flange. To compound the problem, the customer required the use of titanium mounting bolts during test. Since the modulus of titanium is lower than steel 1.1×10^{11} PA versus 2.0×10^{11} PA (16.5×10^6 psi versus 29×10^6 psi), the extra grip length and the bolt size (#8) were a concern. As feared, after a number of setup runs with a dynamic model, several bolts deformed and one bolt snapped at the mounting plane. The use of titanium bolts required a higher ram pressure to achieve a similar shock response as high strength steel bolts. It is believed that the titanium, with a lower elasticity, stiffened the table much more effectively with the component than the steel. The steel bolts would elongate slightly under the shock impulse and would tend to be more forgiving than titanium. The test was successfully completed when the mounting holes were enlarged to accommodate #10 bolts, which were also titanium.

Component D testing was the first attempt to use a transition plate for the MIPS table. Currently, each component is mounted directly to the MIPS plate, which requires an ever increasing amount of holes. Concentrated hole patterns in the plate affect the boundary conditions of the plate, which in turn add a new unknown to the setup. A transition plate for each component would have mounted to a common bolt pattern in the table, thus maintaining the integrity of the setup. The transition plate for Component D was designed to fit an existing hole pattern which

surrounded the component mounting pattern. A 1.3 cm (0.5") thick aluminum plate was used for the adapter. This method was successful, but the setup was difficult due to the effect of this secondary plate. While the MIPS table design was driven by the need to have the plate 'ring' near the crossover point, this secondary plate had its own resonance which made shaping the shock response difficult. For this reason, it was decided to continue with the original method of mounting directly to the large MIPS plate.

Component E was a small passively damped device which required testing in three orthogonal axes. Normally, the MIPS requirement is for the shock to be solely in the plane of the component mounting surface. This test was accomplished by mounting the device in a metal cube, which could be rotated to achieve the three planes. The cube was fabricated from solid steel to provide maximum transmissibility of the shock impulse. The device was not only instrumented with teardrop accelerometers, but also contained mirror cube mounts for collimator readings. Although this method would not be feasible for large components, it has proven to be an alternative for small components requiring three axis shock.

Component F was unique in that it sustained catastrophic internal damage and mounting feet deformation during prior pyro shock testing at another facility. That facility (Figure 8) is quite different than the MIPS facility, thus affecting the path taken by the shock wave from the impact point to the unit. In addition, in the previous test, the flight unit itself was used during system setup with some 67 hits made during the calibration resulting in probable unit over testing. To resolve the question of whether the component failures resulted from being over tested/over exposed or whether the design was susceptible to normal axis shock, another unit was tested at the GE Astro MIPS facility.

The shock spectrum illustration in Figure 9 was applied to the component. The axis definition and instrumentation details for this test are given in Table 3. The control accelerometer was located within 5.1 cm (2") of the mounting foot, and a second reference triaxial accelerometer location was approximately 17.8 cm (7") laterally from the central control as indicated in the figure. All response accelerometers on the component were bonded to tape which was secured to the (flight) unit.

The test sequence consisted of applying three consistent shocks with a dummy in place of the flight unit for calibration, and then a single shock to the flight unit. The procedure was repeated when the unit was rotated 90 degrees. The normal axis input, as measured by station 1 norm, is shown in Table 3 for the XZ test and the YZ test. The three lines in the vicinity of the solid response curve represent the desired levels with +3/-6 dB limits indicated. It is clear that in no band did the response exceed either the +3 or -6 dB limit.

Results of the pyro shock test are summarized in Table 3 with peak time history values tabulated. The unit was exposed to an approximate SRS peak input of 5000 g's in both tests and, upon examination of the test data presented in Table 3, it is clear that the component responses were grossly different between the two test methods. For an approximate normal axis input of 3300 g's, responses at the top of the component for the MIPS test were on the order of 2500 g's, whereas responses with the other Impact Facility illustrated by Figure 8 were some 12,000 g's. It is obvious that the unit as tested on the MIPS assembly experienced grossly lower response levels than experienced on the other test apparatus. The primary difference is due to the path the energy takes before reaching the component and a 200 Hz component response that was magnified by a system resonance with the Impact Facility in the same frequency band. It was

concluded that the MIPS setup is a better representation of the actual environment that the unit will experience in flight and imposes far less structural risk due to the test assembly than the Impact Facility.

CONCLUSION

The MIPS facility provides a unique capability for repeatable shock testing of large components. The manipulation of the boundary conditions allows a wide range of test specifications to be met. Peak levels of 40,000 response g's have been reached with the bare table. The MIPS pyro shock simulator at GE Astro has been used to successfully qualify a variety of components for flight use. Achieving the desired Shock Response Spectrum for different size boxes is a matter of skill and experience, but will always remain an art. This paper presents a few of the 'tricks of the trade' necessary to succeed in using the MIPS. The information presented herein was gathered through the testing of twelve different components. Each component required, on the average, approximately 80 setup shocks on a dynamic model to achieve the proper shock spectrum. As the database grows with each new component, and as communication between MIPS users increases, the setup time and cost can be dramatically reduced.

REFERENCES

- [1] T. J. Dwyer: Design and Dynamic Testing of an Instrumented Spacecraft Component, 58th Shock & Vib Symposium, NASA Conference Publication 2488 Volume II.

TABLE 1: ACCELEROMETER LOCATIONS AND RESPONSES FOR COMPONENT A

Location	Station	XY Axis - Peak SRS		ZY Axis - Peak SRS	
		(g)		(g)	
		Hit 1	Hit 2	Hit 1	Hit 2
Input - Norm	1X	12,930	12,623	1,706	1,808
Input - Long	1Y	6,083	6,131	6,314	6,280
Input - Lat	1Z	1,694	1,902	10,629	10,560
Box Corner	2X	3,406	3,362	4,728	4,623
Box Corner	2Y	5,921	5,761	5,522	5,524
Box Corner	2Z	4,341	4,179	3,147	3,289
PWB - 5	3	873	928	393	458
PWB - 6	4	3,771	--	--	557
PWB - 7	5	--	--	763	650
PWB - 8	6	1,086	1,280	1,207	1,371
PWB - 9	7	1,514	1,654	938	1,043
PWB - 10	8	980	1,248	1,771	1,867
PWB - 11	9	--	--	--	--
PWB - 12	10	1,174	856	1,918	2,007
PWB - 13	11	427	650	532	1,096

TABLE 2: ACCELEROMETER LOCATIONS AND RESPONSES FOR COMPONENT B

Location	Station	XY Axis - Peak SRS		ZY Axis - Peak SRS	
		(g)		(g)	
		Hit 1	Hit 2	Hit 1	Hit 2
Input - Norm	1X	4,000	4,000	4,000	4,000
Input - Long	1Y	4,000	4,000	3,600	3,600
Input - Lat	1Z	850	900	650	750
Box Corner	2X	2,100	2,250	2,250	2,250
Box Corner	2Y	1,000	900	900	900
Box Corner	2Z	--	1,950	1,700	1,650
PWB - 4	4X	550	550	500	550
PWB - 4	4Y	1,100	1,200	550	800
PWB - 4	4Z	350	300	1,000	1,050
PWB - 5	5X	275	300	125	130
PWB - 6	6X	450	375	170	180
PWB - 7	7X	450	450	150	135
PWB - 8	8X	375	360	95	165
PWB - 9	9X	260	270	150	110
PWB - 10	10X	450	500	14	18
PWB - 11	11Y	250	260	500	650

TABLE 3: ACCELEROMETER LOCATIONS AND RESPONSES FOR COMPONENT F

Location	Station	XZ Axis - Peak SRS		ZY Axis - Peak SRS	
		MIPS	(g) Other	MIPS	(g) Other
Control - Lat	1X	800	--	3,400	--
Control - Long	1Y	4,900	--	800	--
Control - Norm	1Z	3,400	3,363	3,200	3,363
Box Corner	2Z	1,900	--	1,700	--
Box Near Impact	3X	500	--	1,100	--
Top Near Impact	4Z	3,400	5,443	2,900	5,443
Top Center	5Z	3,300	11,954	2,500	11,954
Top Away Impact	6Z	2,900	5,443	2,300	5,443
Box Far End	7Y	1,800	--	850	--

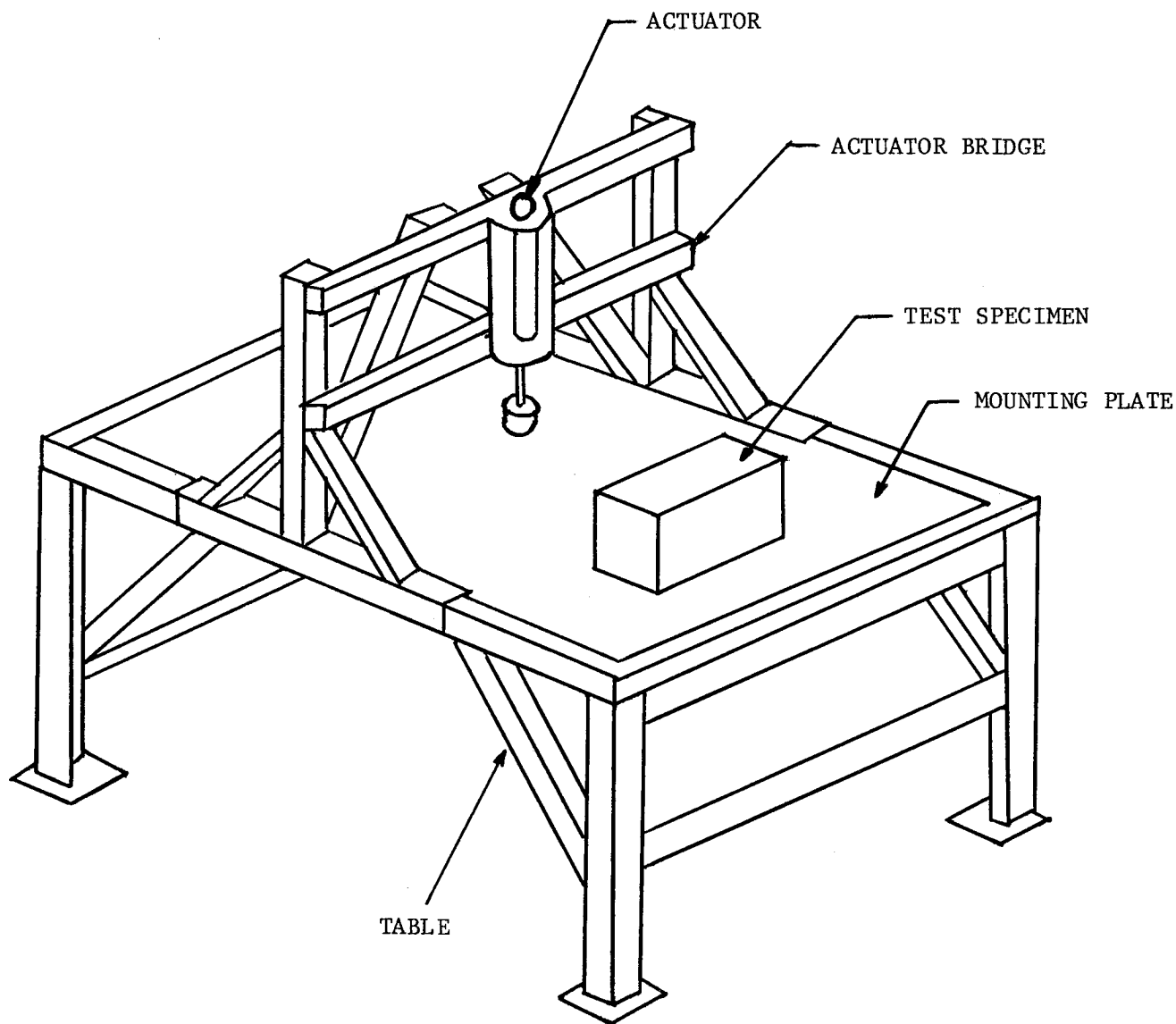
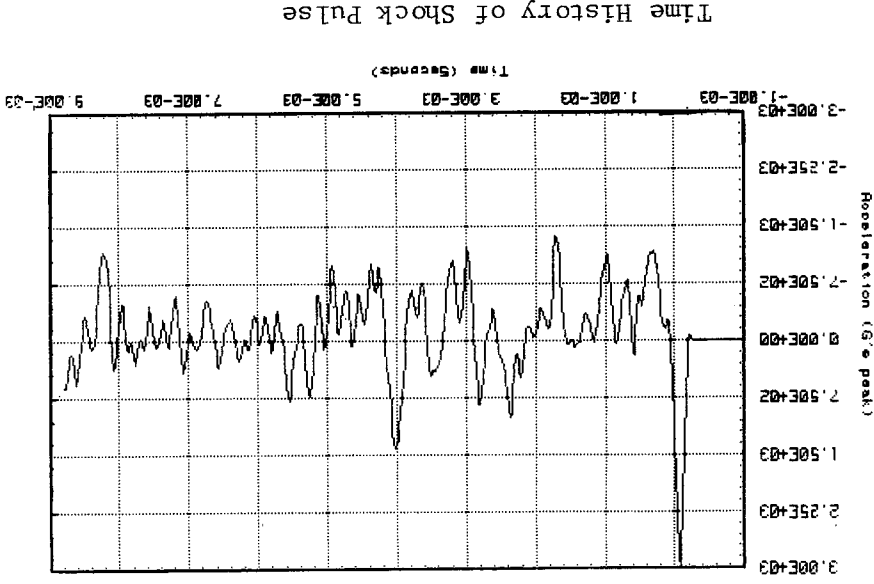
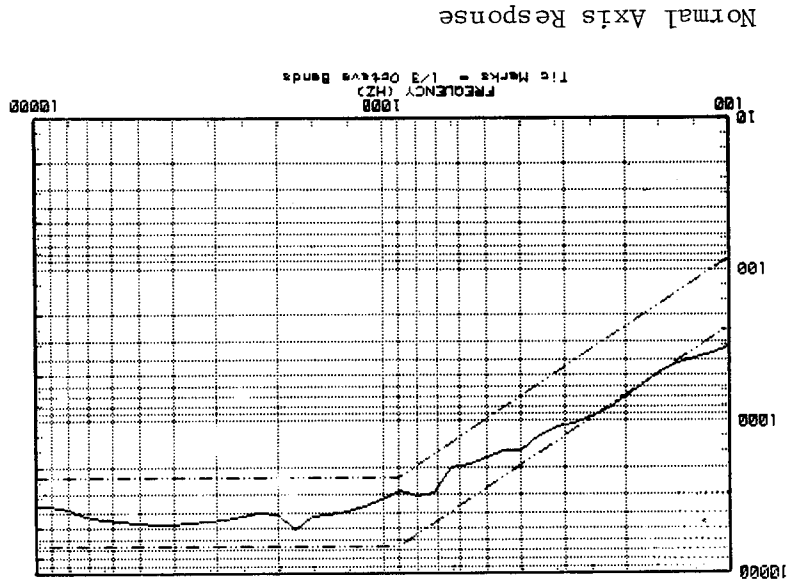
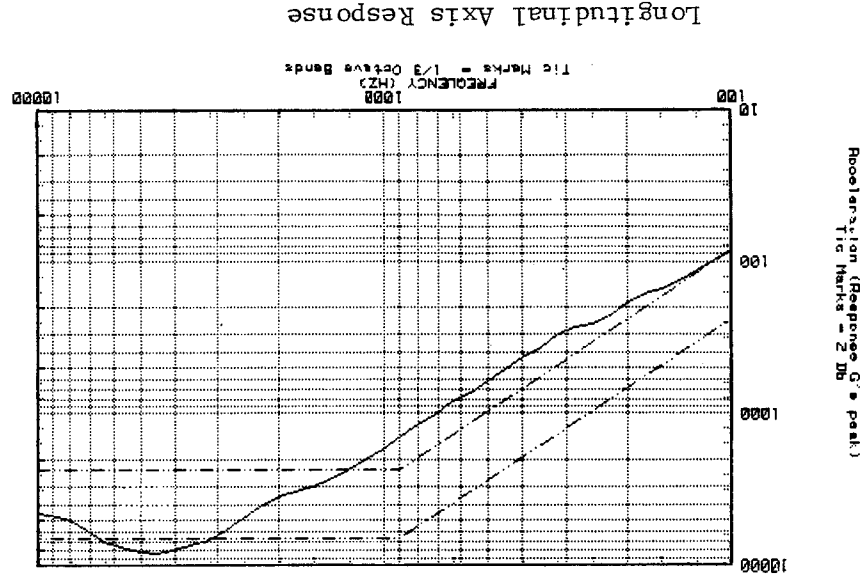
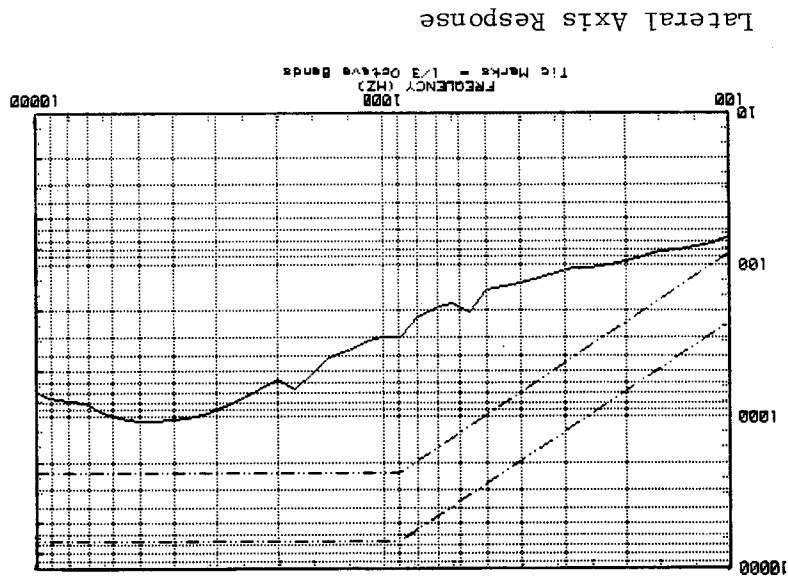


FIGURE 1: GENERAL CONFIGURATION OF MIPS SIMULATOR

FIGURE 2: TYPICAL TRIAXIAL RESPONSE OF CONTROL POINT



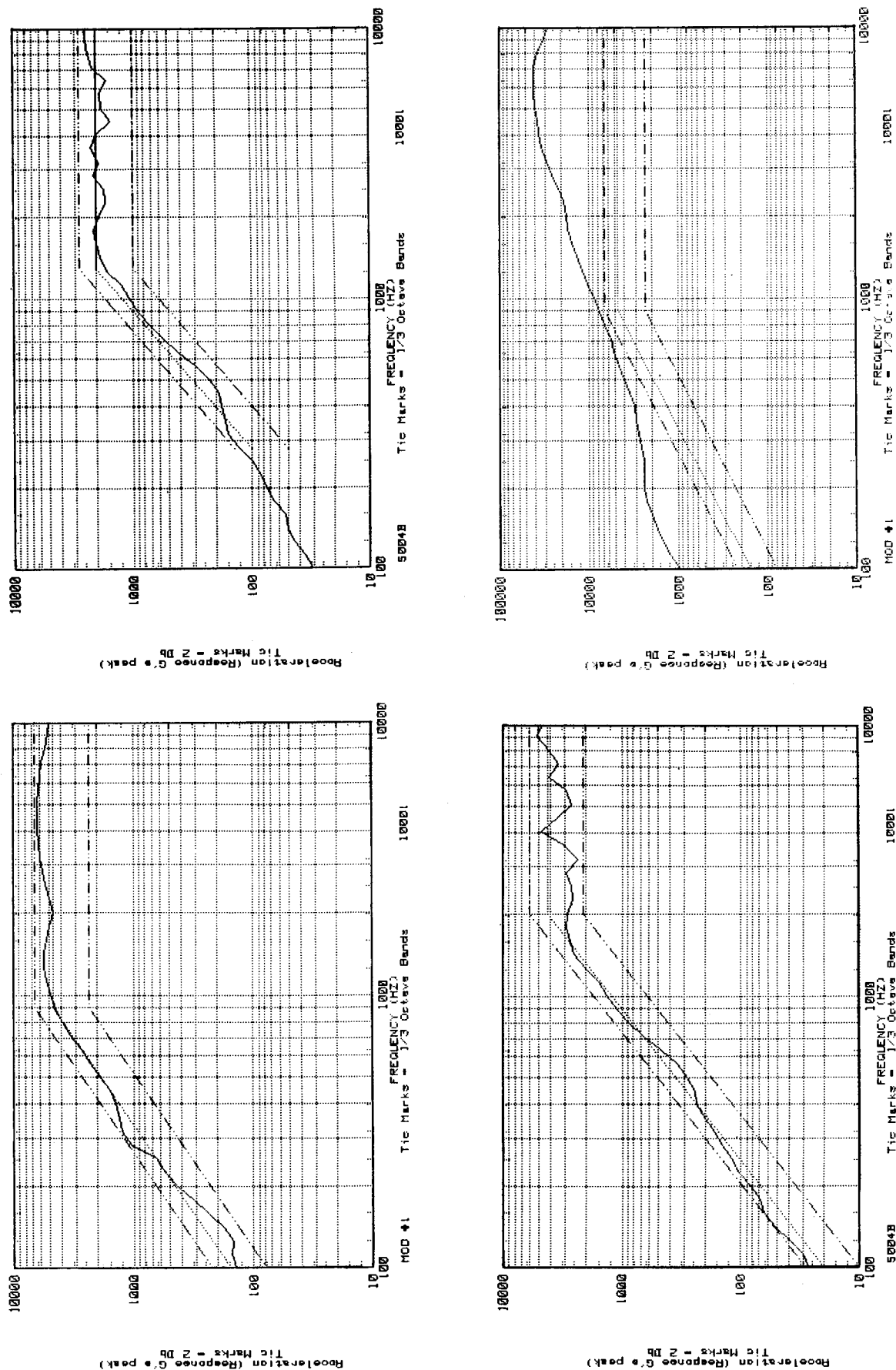
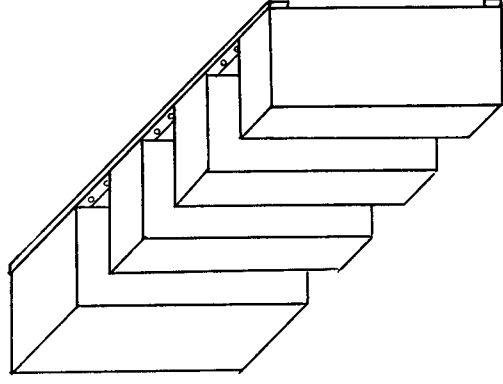
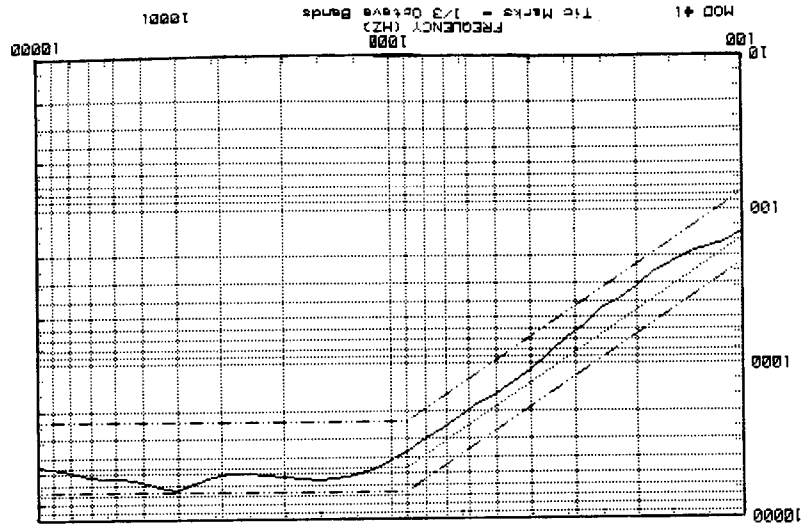


FIGURE 3: FOUR TYPICAL MIPS SHOCK RESPONSE SPECTRA

ORIGINAL PAGE IS
OF POOR QUALITY



Acceleration (Response G's peak)
Tic Marks - 2 dB

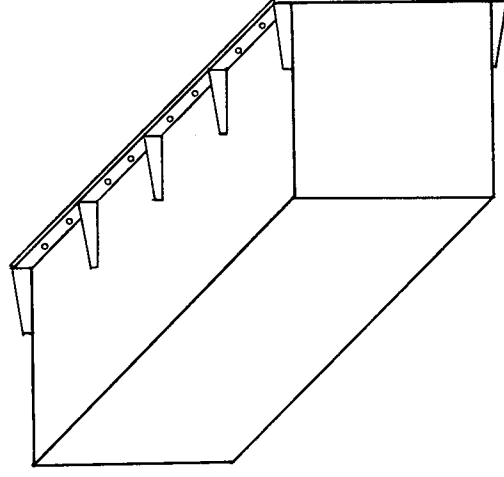
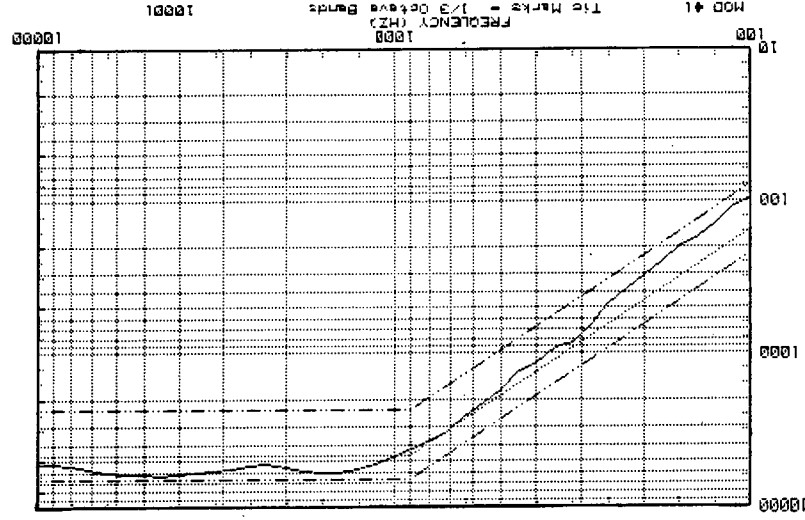
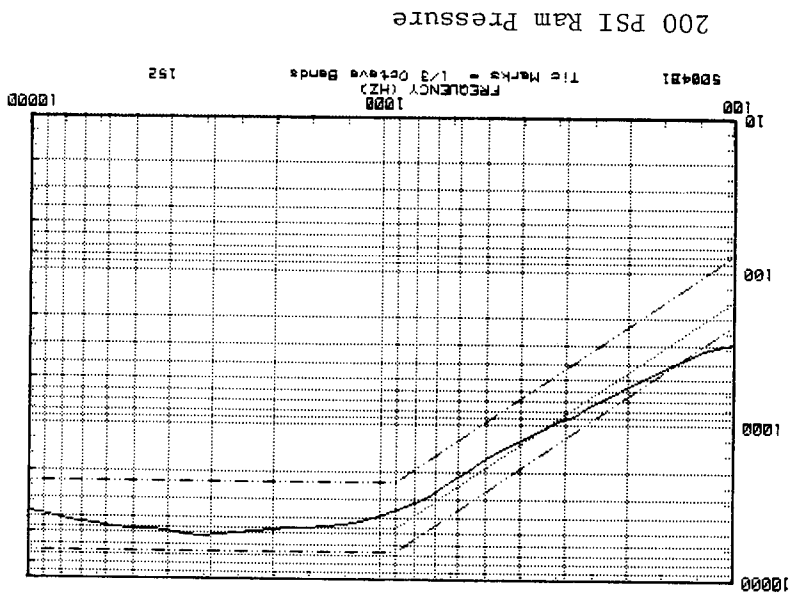


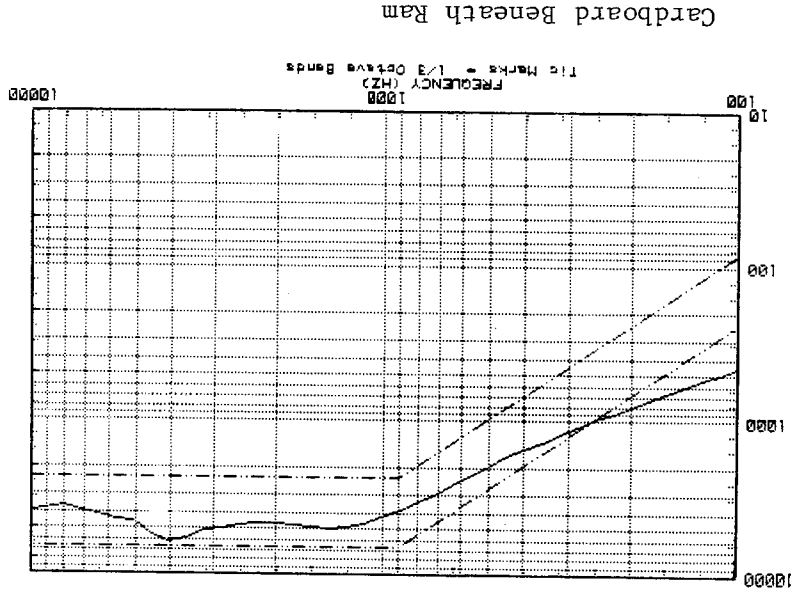
FIGURE 4: COMPARISON OF FLIGHT DESIGN AND TYPICAL DYNAMIC MODEL

Acceleration (Response G's peak)
Tic Marks - 2 dB

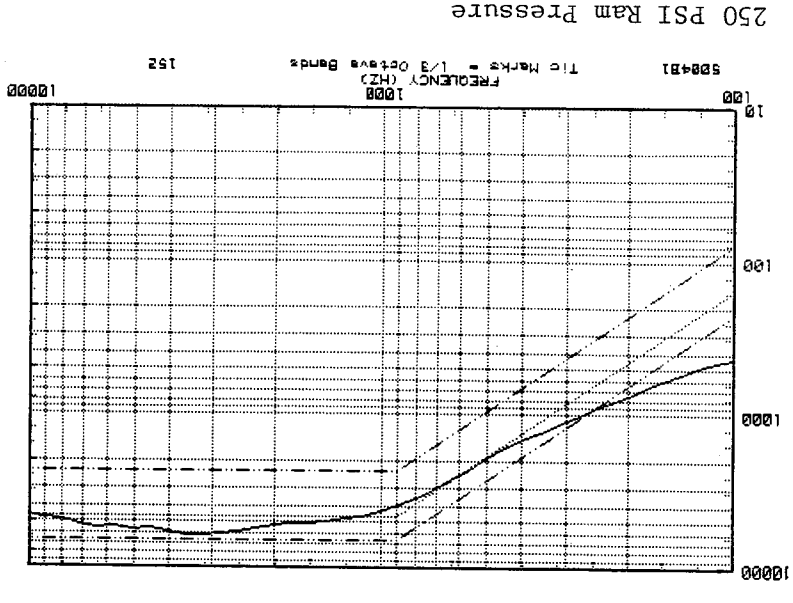
Acceleration (Response G's peak)
Tic Marks = 2 db



Acceleration (Response G's peak)
Tic Marks = 2 db



Acceleration (Response G's peak)
Tic Marks = 2 db



Acceleration (Response G's peak)
Tic Marks = 2 db

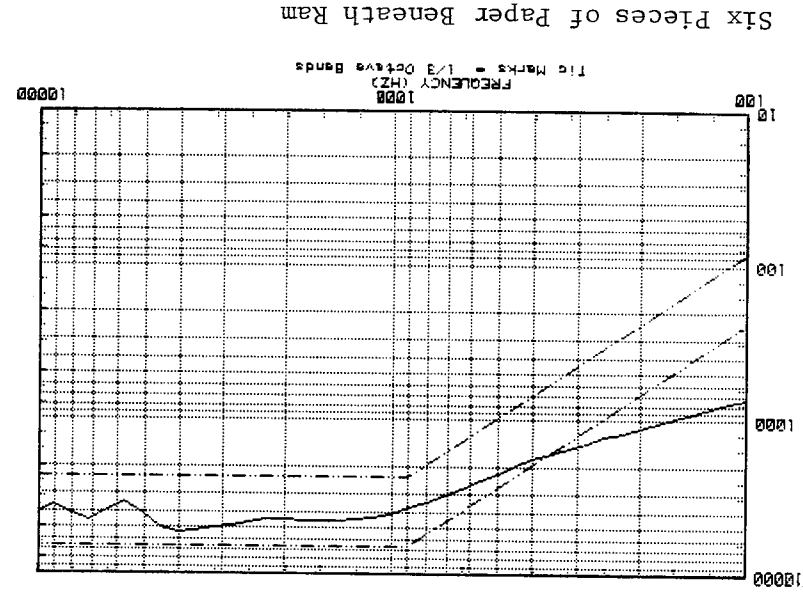


FIGURE 5: SRS COMPARISONS OF FORCE INPUT VARIATIONS

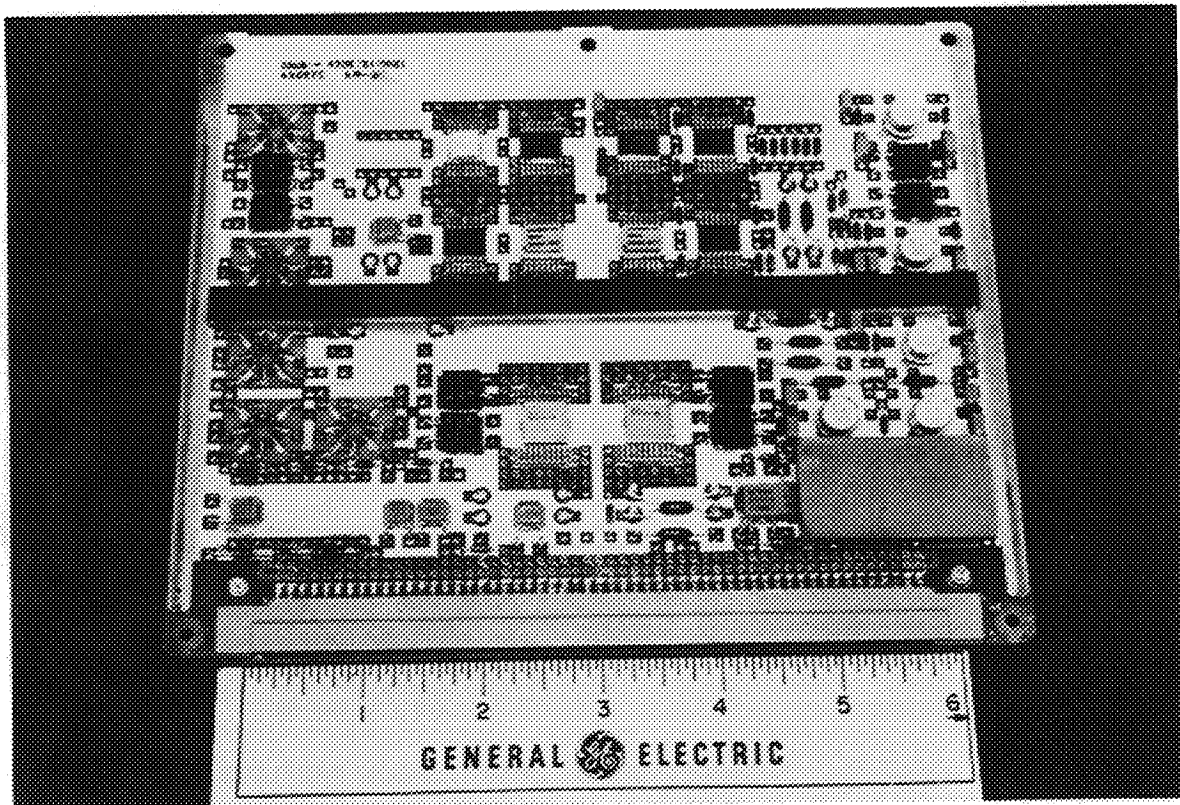


FIGURE 6: TYPICAL PLACEMENT OF CLDA UPON A PWB

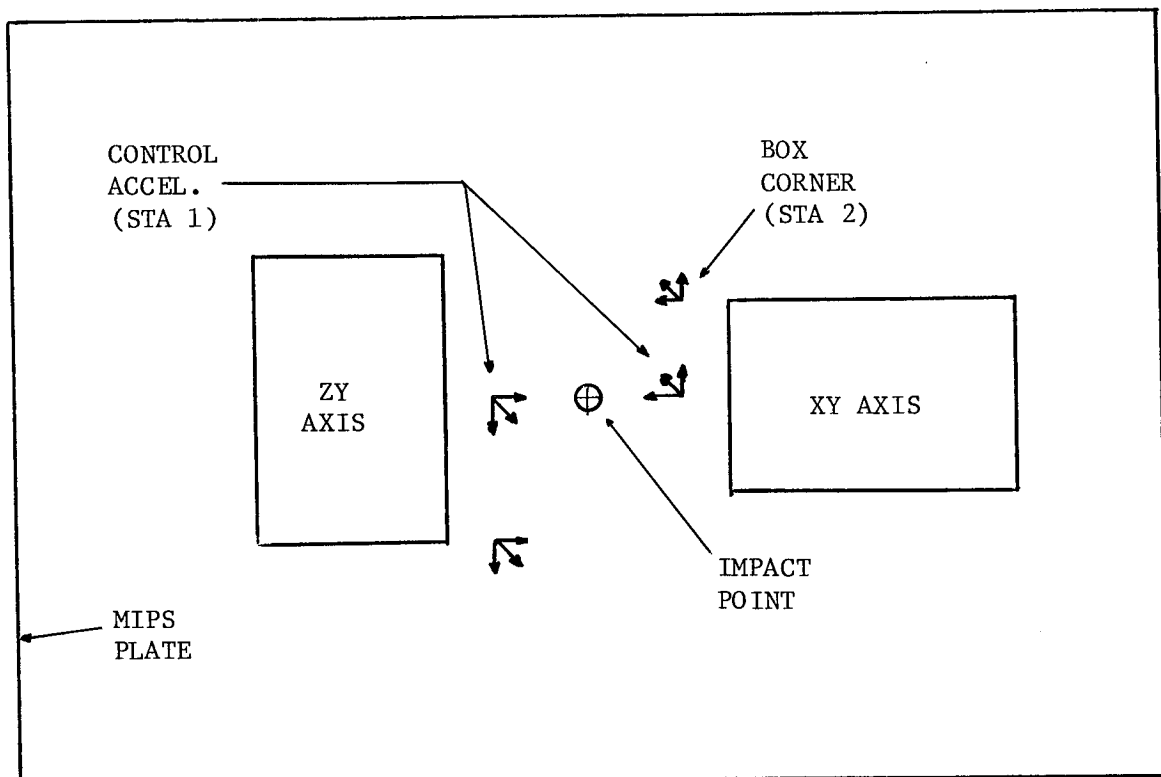


FIGURE 7: TYPICAL TEST GEOMETRY OF BLACK BOX

ORIGINAL PAGE IS
OF POOR QUALITY

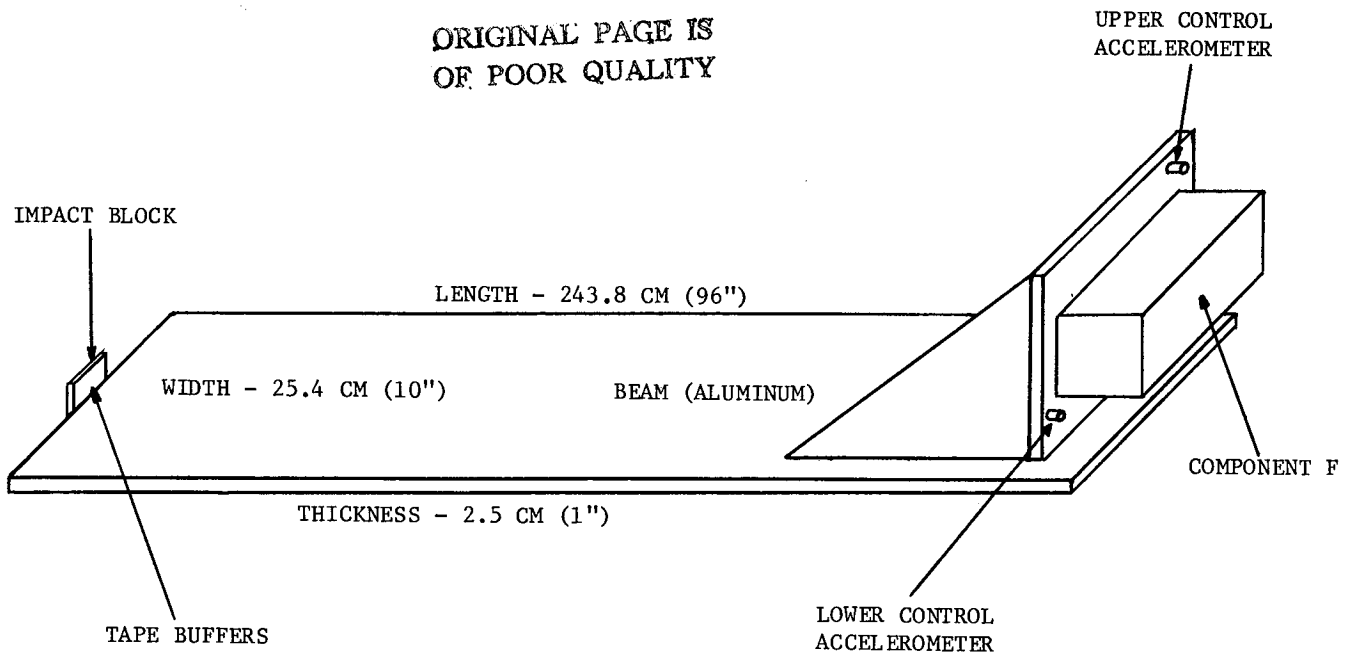


FIGURE 8: NON-EQUIVALENT IMPACT SHOCK FACILITY

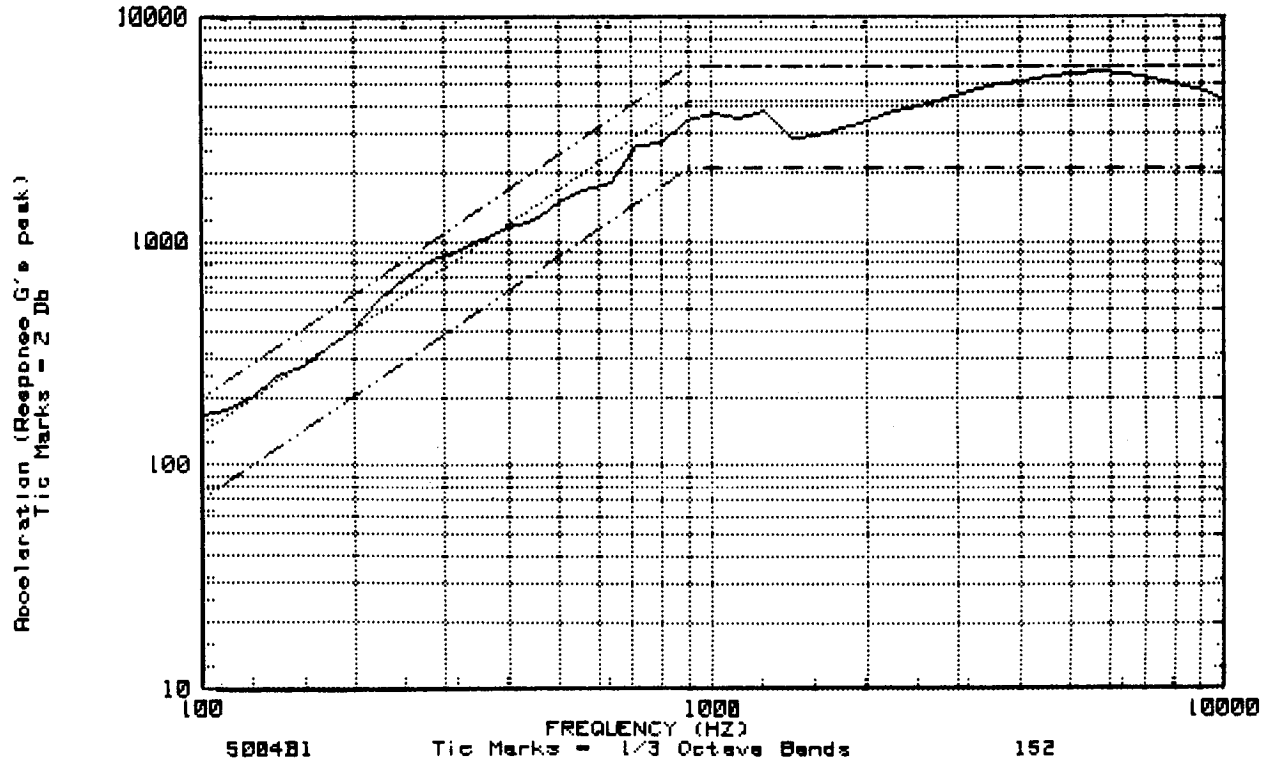


FIGURE 9: COMPONENT F SHOCK SPECTRUM